Sensible and Latent Heat Flux Measurements over the Ocean

W. G. LARGE

National Center for Atmospheric Research,[1] Boulder, CO 80307

S. POND

Department of Oceanography, University of British Columbia, Vancouver, B.C. V6T 1W5, Canada

(Manuscript received 5 October 1981, in final form 13 February 1982)

ABSTRACT

This paper presents an extensive set of sensible heat (Reynolds flux and dissipation methods) and latent heat (dissipation method) flux measurements from a stable deep water tower and from ships on the deep sea. Operational difficulties associated with ship spray and flow distortion and with sensor calibration, response and contamination are discussed. The influence of atmospheric stability on the dissipation measurements and the bulk transfer coefficients is considered and a parameterization of Z/L in terms of wind speed and the sea-air potential temperature difference is found to be adequate. Temperature variances, Stanton numbers and w–t cospectra from the Reynolds flux measurements are compared to previous results.

The dissipation method is shown to be a viable means of measuring the heat fluxes over the deep sea by comparison with simultaneous Reynolds flux measurements, using our data for the sensible heat and the data of others for the latent heat. The neutral drag coefficient at 10 m height, CDN, because it is relatively well established, is used to check the performance of the shipboard measurements. The dissipation sensible and latent heat fluxes are well described, on average, by the neutral transfer coefficients at 10 m height, CTN and CEN, respectively:

$$10^3\,\mathrm{CTN} = 1.13 \quad Z/L < 0, \text{ unstable}, \quad 4 < \mathrm{U10} < 25 \text{ m s}^{-1},$$

$$= 0.66 \quad Z/L > 0, \text{ stable}, \quad 6 < \mathrm{U10} < 20 \text{ m s}^{-1},$$

$$10^3\,\mathrm{CEN} = 1.15 \quad Z/L < 0, \text{ unstable}, \quad 4 < \mathrm{U10} < 14 \text{ m s}^{-1}.$$

Previously published results are considered, indicating that 10^3 CTN = 0.75 may be preferable in stable conditions. Some data suggest a slight wind-speed dependency above 10 m s^{-1}, which is mostly accounted for with CTN and CEN proportional to CDN$^{1/2}$, as implied by constant roughness lengths

$$Z_t = 4.9 \times 10^{-5} \text{ m unstable},$$

$$= 2.2 \times 10^{-9} \text{ m stable},$$

$$Z_q = 9.5 \times 10^{-5} \text{ m unstable}.$$

A bulk aerodynamic method of estimating the heat fluxes from CDN, CTN and CEN, wind speed, sea temperature, and air temperature and humidity is described and compared to time series of the dissipation method heat fluxes. Potential problems with the data are discussed using the time series.

1. Introduction

The turbulent exchange of heat between the ocean and atmosphere is due to sensible heat (temperature) and latent heat (moisture) fluxes. For most purposes direct measurements are too difficult and costly, so parameterizations must be used to estimate the fluxes from more readily available data. Direct, open-ocean and high wind speed measurements are rare, because the most common methods, the Reynolds flux and profile, are not well suited to storm conditions at sea. It is undesirable to extrapolate parameterizations based on near- or on-shore observations to higher wind conditions over the open ocean, so an experimental program was designed to measure fluxes in high winds over the open sea. The dissipation method was employed because it is suitable for shipboard operation during storms at sea.

Initial testing was done in 1975 on the beach of Sable Island, Nova Scotia (Smith *et al.*, 1976). The next experiment lasted from September 1976 to April 1977 on a stable deep water (~60 m depth) tower operated by the Bedford Institute of Ocean-

[1] The National Center for Atmospheric Research is sponsored by the National Science Foundation.

0022-3670/82/050464-19$08.75

ography, BIO, and described in Smith (1980). The data from the Bedford tower have made possible direct comparisons between the Reynolds flux and dissipation methods. The dissipation measurements continued in more open sea and higher wind conditions, during the four patrols of CCGS *Quadra* at ocean weather station "PAPA" between July 1977 and April 1978. The tower and *Quadra* experiments were detailed in Large (1979) and the extensive momentum flux measurements were presented in Large and Pond (1981). During the Joint Air–Sea Interaction Experiment (JASIN 1978) additional temperature and the first successful moisture flux data were recorded from F.S. *Meteor*. An October 1980 cruise of CSS *Parizeau*, in conjunction with the Storm Transfer and Response Experiment (STREX) extended the moisture flux measurements to winds over 10 m s^{-1}.

2. The turbulent fluxes

The turbulent fluxes are most easily measured in the atmospheric surface layer, whose behavior is well described by Monin-Obukhov similarity theory. Hasse *et al.* (1978) found that the wave influence on the mean wind profile is confined mainly to heights comparable to the wave height. Above such direct influences of the bottom boundary, the important parameters are the height Z, the mean air density ρ and the turbulent transports through the layer. These transports are the Reynolds fluxes:

$$\left.\begin{aligned} &\text{momentum flux (surface stress)} \quad \tau = -\rho\langle uw\rangle \\ &\text{sensible heat flux} \quad H_s = \rho C_p\langle wt\rangle \\ &\text{latent heat flux} \quad H_L = L_E\langle wq\rangle \end{aligned}\right\}, \tag{1}$$

where C_p is the specific heat at constant pressure of dry air (Businger, 1982) and L_E is the latent heat of evaporation. Following Reynolds' convention the downstream and vertical velocity components, the air temperature and absolute humidity (water vapor density) are partitioned into a mean [$\langle\ \rangle$, time average] and fluctuation (lower case), such that they become $\langle U\rangle + u$, $\langle W\rangle + w$, $\langle T\rangle + t$ and $\langle Q\rangle + q$, respectively. The kinematic fluxes $\langle wt\rangle$ and $\langle wq\rangle$ are, respectively, the temperature flux and the moisture flux excluding liquid water, which arises from evaporation both at the sea surface and of spray in the atmosphere. Other relevant quantities are the sea surface temperature T_s, the absolute humidity at the surface Q_s, and the potential temperature θ, where $\langle\theta\rangle = \langle T\rangle + \gamma Z$, with γ the adiabatic lapse rate 0.01 K m^{-1}.

The supposed height independence of the fluxes leads naturally to the following scales

$$\left.\begin{aligned} &\text{friction velocity:} \\ &\quad u^* = (\tau/\rho)^{1/2} = |\langle uw\rangle|^{1/2} \\ &\text{temperature scale:} \\ &\quad t^* = -\langle wt\rangle(\kappa u^*)^{-1} \text{ or } T^* = -\langle wt\rangle u^{*-1} \\ &\text{humidity scale:} \\ &\quad q^* = -\langle wq\rangle(\kappa u^*)^{-1} \text{ or } Q^* = -\langle wq\rangle u^{*-1} \\ &\text{Monin-Obukhov length:} \\ &\quad L = -u^{*3}T_0(\kappa g\langle wT_v\rangle)^{-1} \end{aligned}\right\}, \tag{2}$$

where κ is von Kármán's constant (0.40, Busch, 1977), g is gravitational acceleration and T_v is the virtual temperature in degrees Kelvin, with $\langle wT_v\rangle$ its vertical flux and T_0 its local average. Similarity theory predicts that mean gradients are universal functions of the stability parameter Z/L:

$$\left.\begin{aligned} \frac{\kappa Z}{u^*}\frac{\partial\langle U\rangle}{\partial z} &= \phi_m(Z/L) \\ \frac{Z}{t^*}\frac{\partial\langle\theta\rangle}{\partial z} &= \phi_t(Z/L) \\ \frac{Z}{q^*}\frac{\partial\langle Q\rangle}{\partial z} &= \phi_q(Z/L) \end{aligned}\right\}. \tag{3}$$

Integration of (3) gives the mean quantities at a height Z

$$\left.\begin{aligned} UZ &= u^*\kappa^{-1}[\ln(Z/Z_0) - \psi_m(Z/L)] \\ \theta Z &= T_s + t^*[\ln(Z/Z_t) - \psi_t(Z/L)] \\ QZ &= Q_s + q^*[\ln(Z/Z_q) - \psi_q(Z/L)] \end{aligned}\right\}, \tag{4}$$

with

$$\psi(Z/L) = \int_0^{Z/L} \frac{[1 - \phi(\zeta)]}{\zeta}\, d\zeta, \tag{5}$$

except at small Z when the logarithms of $(Z + Z_0)/Z_0$, $(Z + Z_t)/Z_t$ and $(Z + Z_q)/Z_q$ must be used. The constants of integration Z_0, Z_t and Z_q are the surface roughness lengths for momentum, temperature and humidity, respectively.

Reviews of the flux-profile relationships (3) (Dyer, 1974; Yaglom, 1977) indicate that reasonable forms are

$$\left.\begin{aligned} \phi_m &= 1 + C_1 Z/L \\ \phi_t = \phi_q &= 1 + C_2 Z/L \end{aligned}\right\}, \quad 0 < Z/L < 0.2,$$

$$\left.\begin{aligned} \phi_m &= (1 - C_3 Z/L)^{-1/4} \\ \phi_t = \phi_q &= (1 - C_4 Z/L)^{-1/2} \end{aligned}\right\}, \quad -1.0 < Z/L < 0. \tag{6}$$

In the unstable case, the constants are likely in the ranges $16 \leqslant C_3 \leqslant 22$ and $13 \leqslant C_4 \leqslant 16$, throughout which $\phi_m(-1.0)$ and $\phi_t(-1.0)$ only change by 6 and

10%, respectively. There is more sensitivity to the choices of C_1 and C_2, which appear to be in the ranges $5 < C_1 < 7$ and $5 < C_2 < 10$. A value of $C_1 = 5$ was used in Large and Pond (1981), but it was noted that $C_1 = 7$ gave better agreement between Reynolds flux and dissipation momentum fluxes. The corresponding $\langle wt \rangle$ comparison in Section 4, indicates that the mid-range value $C_2 = 7$ is a good choice. Comparisons of $\langle wq \rangle$ and $\langle wt \rangle$ from the two techniques at BIO, using Sable Island data, show $C_2 = 7$ to give better agreement than $C_2 = 5$ (R. J. Anderson, pers. comm., 1981). With $C_3 = C_4 = 16$ and $C_1 = C_2 = 7$, (5) becomes (Paulson, 1970)

$$\left.\begin{aligned} \psi_m(Z/L) &= \psi_t(Z/L) = \psi_q(Z/L) = -7Z/L, && \text{stable} \\ \psi_m(Z/L) &= 2\ln[(1+X)/2] + \ln[(1+X^2)/2] - 2\tan^{-1}X + \pi/2 && \\ \psi_t(Z/L) &= \psi_q(Z/L) = 2\ln[(1+X^2)/2], && \text{unstable} \\ \text{with } X &= (1 - 16\,Z/L)^{1/4} && \end{aligned}\right\}. \tag{7}$$

a. The bulk aerodynamic method

The bulk aerodynamic formulas parameterize the kinematic fluxes in terms of the more easily measured mean or bulk quantities (Roll, 1965)

$$\left.\begin{aligned} -\langle uw \rangle \text{BULK} &= \text{CD}\, UZ^2 \\ \langle wt \rangle \text{BULK} &= \text{CT}\, UZ\, \Delta\theta \\ \langle wq \rangle \text{BULK} &= \text{CE}\, UZ\, \Delta Q \end{aligned}\right\}, \tag{8}$$

where $\Delta\theta = T_s - \theta Z$ and $\Delta Q = Q_s - QZ$. The non-dimensional transfer coefficients CD, CT and CE are the drag coefficient, Stanton number and Dalton number, respectively. They are functions of height and stability and commonly evaluated in the equivalent neutral case at 10 m as

$$\left.\begin{aligned} \text{CDN} &= \kappa^2/[\ln(10/Z_0)]^2 \\ \text{CTN} &= \kappa^2/[\ln(10/Z_0)\ln(10/Z_t)] \\ \text{CEN} &= \kappa^2/[\ln(10/Z_0)\ln(10/Z_q)] \end{aligned}\right\}, \tag{9}$$

with Z_0, Z_t and Z_q in meters.

Empirical formulations of CDN, CTN, and CEN allow the turbulent heat fluxes to be estimated from UZ, θZ or TZ, QZ and T_s using (1) and (8). The saturation humidity (g m^{-3}) over pure water at T degrees Kelvin is $Q\text{SAT}(T) \approx 64038 \times 10^4 \exp \times (-5107.4/T)$, and over salt water is $Q_s \approx 0.98\, Q\text{SAT}(T_s)$. Following Deardorff (1968), but allowing the coefficients (9) to differ and retaining the height dependency, (4) and (9) give, for Z and L in meters,

$$\text{CT} = \frac{\text{CTN}\,(\text{CD/CDN})^{1/2}}{1 + \text{CTN}\kappa^{-1}\text{CDN}^{-1/2}[\ln(Z/10) - \psi_t(Z/L)]},$$

$$\text{CE} = \frac{\text{CEN}\,(\text{CD/CDN})^{1/2}}{1 + \text{CEN}\kappa^{-1}\text{CDN}^{-1/2}[\ln(Z/10) - \psi_q(Z/L)]}, \tag{10}$$

where

$$(\text{CD/CDN})^{1/2} = \{1 + (\text{CDN})^{1/2}\kappa^{-1}[\ln(Z/10) - \psi_m(Z/L)]\}^{-1}.$$

When CDN is given as a function of the 10 m wind, U10,

$$\text{UZ/U10} \approx 1 + (\text{CDN})^{1/2}\kappa^{-1} \times [\ln(Z/10) - \psi_m(Z/L) + \psi_m(10/L)],$$

is quickly solved iteratively for U10 and CDN. Large errors in CT and CE (and hence in $\langle wt \rangle$BULK and $\langle wq \rangle$BULK) come from uncertainties in CTN and CEN, up to 10 and 20%, respectively. In the range $-0.30 < Z/L < 0.15$, $\psi_t(Z/L)$ ranges from 1.0 to -1.0, and assuming neutral stability ($Z/L = 0$) leads to an additional 20% error at these extremes (and nearly 40% at $Z/L = -1.0$ and 0.20).

This error can be significantly reduced by using a bulk estimate, $Z/L(\Delta\theta)$, based on $\Delta\theta$ and the most recent determinations of the bulk coefficients. Expanding (2) gives, for q in (g m^{-3}),

$$Z/L(u^*, \langle wt \rangle, \langle wq \rangle) = \frac{-\kappa Z g}{u^{*3} T_0}(\langle wt \rangle + 1.7 \times 10^{-6} T_0^2 \langle wq \rangle). \tag{11}$$

Often the moisture flux is unknown, and a stability estimate is

$$Z/L(u^*, \langle wt \rangle) = \frac{-\kappa Z g}{u^{*3} T_0}\langle wt \rangle\left(1 + 1.7 \times 10^{-6} T_0^2 \frac{\text{CE}}{\text{CT}}\frac{\Delta Q}{\Delta\theta}\right), \tag{12}$$

though care must be taken at small $\Delta\theta$. At the lower wind speeds where Z/L is largest, CD $= 1.2 \times 10^{-3}$ is a reasonable average (Large and Pond, 1981). Smith (1980) and Large (1979) show that CT is about 1.1×10^{-3} in unstable and 0.75×10^{-3} in

stable stratification. A similar dependency is not observed in CE (Anderson and Smith, 1981), which does not appear to be very different than that of the unstable CT. Substituting (8) and these values into (11) gives

$$\left.\begin{aligned} Z/L(\Delta\theta) &\approx \frac{-100Z}{(UZ)^2T_0}(\Delta\theta + 1.7\times10^{-6}T_0^2\Delta Q), \quad \Delta\theta > 0, \quad \text{unstable} \\ &\approx \frac{-70Z}{(UZ)^2T_0}(\Delta\theta + 2.5\times10^{-6}T_0^2\Delta Q), \quad \Delta\theta < 0, \quad \text{stable} \end{aligned}\right\}, \tag{13}$$

where $T_0 \approx TZ[1 + 1.7 \times 10^{-6}TZ\ QZ]$ and, assuming a 75% relative humidity, $\Delta Q \approx 0.98\ Q\text{SAT}(T_s) - 0.75Q\text{SAT}(TZ)$. Deardorff's (1968) formulation is similar, but the numerical constants at all stabilities are ~118 (instead of 100 or 70) and 1.7×10^{-6}.

The turbulent heat fluxes are sometimes parameterized as

$$\left.\begin{aligned} \langle wt\rangle &= a_tU10(T_s - \theta 10) + b_t \\ \langle wq\rangle &= a_qU10(Q_s - Q10) + b_q \end{aligned}\right\}, \tag{14}$$

where the a's and b's are the slopes and offsets, respectively, of linear regressions. Often the transfer coefficients CT and CE are equated to the slopes a_t and a_q, respectively.

b. The Reynolds flux method

The Reynolds flux or eddy correlation method is the most direct, and hence standard, means of measuring the turbulent fluxes and evaluating the coefficients of (8), (9) and (14). We found $\langle uw\rangle$, $\langle wt\rangle$, and $\langle wq\rangle$ by integrating the cospectra, $\Phi_{uw}(f)$, $\Phi_{wt}(f)$ and $\Phi_{wq}(f)$, over *all* contributing frequencies, f. Briefly, low frequency Fourier coefficients were obtained by sampling at the slow rate of ⅓ Hz. In order to conserve power and recording capacity, the high frequencies were subsampled at the somewhat faster rate of 3 Hz. By allowing frequencies above the Nyquist frequency (1.5 Hz) to alias back to sampled frequencies, most of the contributions to the variances and covariances below $f_n \simeq 4$ Hz were accounted for. As a consequence, the cospectra were distorted above ~0.5 Hz.

Some variability in flux calculations arises because the low frequency contributions are not well sampled. This problem was minimized by integrating the cospectra starting at different frequencies f_1, which always corresponded to the same natural frequency $n_1 = f_1Z/\langle U\rangle = 0.004$, then multiplying by a factor E to compensate for the lower frequencies. Using the temperature flux as an example, the eddy correlation calculations were

$$\langle wt\rangle\text{FLUX} = E\int_{f_1}^{f_n}\Phi_{wt}(f)df,$$

where

$$E = \frac{\int_0^{n_2}N\Phi_{wt}(n)d(\log n)}{\int_{n_1}^{n_2}N\Phi_{wt}(n)d(\log n)}. \tag{15}$$

The normalized cospectrum $N\Phi_{wt}(n)$ was formed by averaging all discrete values of

$$f\cdot\Phi_{wt}(f)\Big/\int_{f_1}^{f_n}\Phi_{wt}(f)df = n\cdot\Phi_{wt}(n)\Big/\int_{f_1}^{f_n}\Phi_{wt}(f)df$$

in bands of $\log(n)$, with $n = fZ\langle U\rangle^{-1}$. It is a universal function of Z/L, so high wind speed runs gave its low-frequency behavior. From the low wind speed runs, with aliasing, the upper limit of integration n_2 was ~10.

c. The dissipation method

The most attractive feature of the dissipation method is that it avoids an explicit measurement of the vertical velocity. The problem of evaluating the heat fluxes is transformed to finding u^* and the dissipation rates of $\langle t^2\rangle/2$ and $\langle q^2\rangle/2$, N_t and N_q, respectively. In steady, horizontal homogeneous flow the scalar variance budgets are (Busch, 1977)

$$\left.\begin{aligned} 0 &= -\langle wt\rangle\frac{\partial\langle\theta\rangle}{\partial z} - N_t - \frac{1}{2}\frac{\partial}{\partial z}\langle wt^2\rangle \\ 0 &= -\langle wq\rangle\frac{\partial\langle\theta\rangle}{\partial z} - N_q - \frac{1}{2}\frac{\partial}{\partial z}\langle wq^2\rangle \end{aligned}\right\}. \tag{16}$$

Assuming that the vertical divergence terms are negligible and substituting (2) and the profile relationships (3) yields

$$\left.\begin{aligned} \langle wt\rangle\text{DISS} &= [\kappa Zu^*N_t/\phi_t(Z/L)]^{1/2} \\ \langle wq\rangle\text{DISS} &= [\kappa Zu^*N_q/\phi_q(Z/L)]^{1/2} \end{aligned}\right\}, \tag{17}$$

where the sign of the square root is the sign of $\Delta\theta$ or ΔQ, respectively. Large and Pond (1981) established that the analogous dissipation method is a viable means of estimating u^* and the momentum flux

$$(u^*\text{DISS})^3 = \kappa Z\epsilon[\phi_m(Z/L) - Z/L]^{-1}, \tag{18}$$

where ϵ is the rate of molecular dissipation of tur-

bulent kinetic energy. Direct measurements of ϵ, N_t and N_q over the sea are very difficult, because they involve centimeter scales (frequencies above 100 Hz). However, they can be inferred from spectral density estimates of the downstream velocity, air temperature and the absolute humidity [$\Phi_u(f)$, $\Phi_t(f)$ and $\Phi_q(f)$, respectively] at frequencies where the Kolmogoroff hypothesis predicts $f^{-5/3}$ spectral behavior:

$$\left.\begin{aligned}\Phi_u(f) &= K'\epsilon^{2/3}(2\pi/\langle U\rangle)^{-2/3}f^{-5/3}\\ \Phi_t(f) &= \beta_t'\epsilon^{-1/3}N_t(2\pi/\langle U\rangle)^{-2/3}f^{-5/3}\\ \Phi_q(f) &= \beta_q'\epsilon^{-1/3}N_q(2\pi/\langle U\rangle)^{-2/3}f^{-5/3}\end{aligned}\right\}, \quad (19)$$

where Taylor's hypothesis has replaced the downstream radian wavenumber with $(2\pi f/\langle U\rangle)$. The $f^{-5/3}$ regions of these spectra have been observed to lie at natural frequencies above $n_0 = 0.2$, 0.6 and 0.2, respectively (Pond *et al.*, 1971; Phelps and Pond, 1971), even though isotropic turbulence occurs only at higher frequencies. Acceptable values for the one-dimensional Kolmogoroff constants are $K' = 0.55$, $\beta_t' = 0.80$ and $\beta_q' = 0.80$ (Paquin and Pond, 1971; Busch, 1977), with ~10% uncertainties.

Evidence for the above assumptions comes from investigations over land, usually in unstable stratification. In the temperature variance budget, Wyngaard and Coté (1971) found the vertical divergence term to be an order of magnitude smaller than the production term $\langle wt\rangle\partial\langle\theta\rangle/\partial z$, and both inhomogeneities and time dependencies to be negligible. Bradley *et al.* (1981) found the divergence term to be negligible compared to both the production and dissipation terms, which themselves nearly balanced in near-neutral conditions. An imbalance for moderately unstable conditions was attributed to an underestimation of N_t. In two of the four runs (2 and 3) reported in Champagne *et al.* (1977), there was a balance between production and dissipation in both budgets (16), with N_q calculated from (19) with β_q' $\approx$ 0.8. However, they balanced the moisture variance budget, averaged over all four runs, by using β_q' $\simeq$ 1.0 and they discuss several possible contributors to the observed imbalances, especially in the temperature variance budget (runs 1 and 4). In Bradley *et al.* (1981) and Champagne *et al.* (1977), N_t was calculated from direct measurements of $\partial\theta/\partial t$ (assuming isotropy and Taylor's hypothesis) and β_t' was found to be ~0.8 and 0.82 $\pm$ 0.04, respectively. Williams and Paulson (1977) found β_t' to be ~0.9 at low frequencies (with uncertainties as large as $\pm$0.2) and greater than 1.2 at higher frequencies.

The vertical fluxes (17) can be calculated from expressions of the form

$$\langle wq\rangle\text{DISS} = S_E[\Phi_u(f)\Phi_q(f)]^{1/2}U^{-2/3}$$

with

$$S_E = [K'\beta_q'\phi_q(Z/L)]^{-1/2}(2\pi\kappa Z)^{2/3} \times f^{5/3}[\phi_m(Z/L) - Z/L]^{-1/6}, \quad (20)$$

which can be regarded as a parameterization of the fluxes in terms of a wind speed and high frequency fluctuations. The foregoing theory and experiments predict the value and stability dependence of the coefficient S_E and its $\langle wt\rangle$DISS analogue S_T. However, the forms of (3), (16) and (19), the values of the constants and the Taylor hypothesis are not well established over the sea, so direct comparisons with eddy correlation measurements are essential. Eq. (20) is particularly well suited to shipboard applications, because the ship's speed need not be removed from the relative wind speed U and reasonably robust sensors will respond to the required frequencies, which are above those contaminated by ship motion. Measurements of true wind speed, mean air and sea temperature and humidity are required only for estimating a bulk Z/L and evaluating the transfer coefficients of (8), (9) and (14).

In our dissipation system each sensor signal was sent through three band-pass filters, centered nominally at $f_c = 0.4$, 0.8 and 1.6 Hz, with effective low-frequency cut-offs at $f_L = 0.3$, 0.6 and 1.2 Hz, respectively. These frequencies correspond to a narrow low-frequency range of the Williams and Paulson (1977) measurements, where β_t' is approximately constant. The power from these filters averaged over at least 20 min was used to estimate the spectral densities $\Phi_u(f_c)$, $\Phi_t(f_c)$, $\Phi_q(f_c)$, and hence $\epsilon(f_c)$, $N_t(f_c)$, $N_q(f_c)$. The dissipation rates ϵ, N_t and N_q were taken to be the averages of $\epsilon(f_c)$, $N_t(f_c)$ and $N_q(f_c)$ from only those filters entirely in the $-5/3$ region, $n_0 < f_L Z/\langle U\rangle$. A symptom of some unreliable data (wake effects, radio interference) was the loss of the $f^{-5/3}$ region; therefore, all data were checked to ensure that all spectral values fell within 10% of an "average" $-5/3$ slope. Thus, if any $\epsilon(f_c)$ with $f_L > (n_0\langle U\rangle/Z)$ differed from the average ϵ by more than 15%, no fluxes were computed. In addition, if any of the $N_t(f_c)[N_q(f_c)]$ with $f_L > (n_0\langle U\rangle/Z)$ differed from the average $N_t(N_q)$ by more than 10% the temperature (moisture) flux was not calculated.

3. The experiments

The instrumentation, including error analysis, design criteria and sensor requirements, is fully described in Pond and Large (1978) and Large (1979). In addition, the velocity measurements (based on a Gill propeller-vane anemometer) are described in detail in Pond *et al.* (1979) and briefly in Large and Pond (1981). Ship velocities (or positions) were usu-

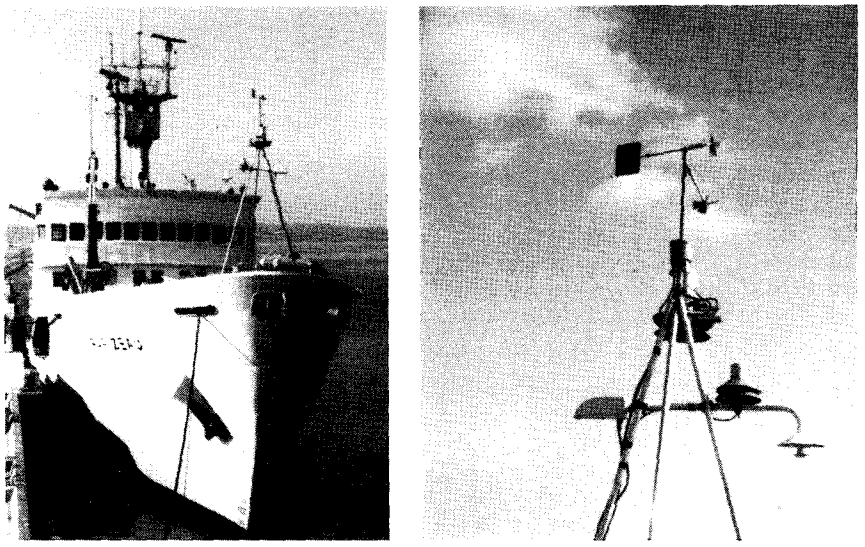

FIG. 1. Sensors above the bow of CSS *Parizeau*. From the top are the Gill twin propeller-vane anemometer, the enclosure for the temperature sensors, the Lyman-alpha humidiometer and the dewpoint system.

ally recorded by the ship's personnel and removed vectorially from the Gill velocities. They were supplemented on the first half of the *Parizeau* cruise by the positions of satellite-tracked drifting buoys stored on deck. Fig. 1 shows the arrangement of the sensors above the bow of CSS *Parizeau*. From top to bottom are the Gill anemometer, ~12 m above the mean water line, an enclosure for the temperature sensors and the Lyman-alpha humidiometer (Electromagnetic Research Corporation) clamped atop a Cambridge Systems (Model 2000) dewpoint system at 10 m.

a. The temperature measurement

The air temperature and its fluctuations were measured with glass-coated microbead thermistors, while glass rod thermistors potted in soft epoxy gave a mean air temperature and the sea-surface temperature at the Bedford tower (~10 m below mean sea level). During ship operations sea-surface bucket temperatures were recorded. In the field the rods provided a continuous *in situ* check on the microbead calibration and whenever the difference in hourly means exceeded 0.1°C the data were rejected.

The humidity sensitivity of salt-contaminated microbeads (Schmitt *et al.*, 1978) must be recognized and the data rejected since they cannot be corrected. It is easily noticed in Reynolds flux data, because a symptom is relatively little variance in the temperature spectrum below $n \simeq 0.01$ compared to higher frequencies. Usually the $f^{-5/3}$ region is lost; however, these higher frequencies occasionally exhibit nearly $f^{-5/3}$ behavior over the narrow range of the $\Phi_t(f_c)$ measurements. In such cases, dissipation data alone do not reveal the microbead contamination, which results in erroneously high values of $\langle wt \rangle$DISS. Therefore, at three-hour intervals on both the tower and ships, the temperature spectrum from the Reynolds flux data was checked and whenever a relatively large variance was found at high frequencies, the dissipation data were rejected.

The air temperature sensor enclosure served as a radiation shield and as protection from rain and spray. On the Bedford tower it was located near the Gill anemometer at ~12 m height. It was mounted on the foremast of CCGS *Quadra* near the other sensors at ~21 m height and 15 m aft of the bow, where bow-generated spray soon broke the microbeads. During JASIN, similar enclosures were installed near Gill anemometers both at 21 m on a mast above the bridge of F.S. *Meteor* and at 8 m on a boom extending ~10 m out from the bow. The microbead survival was much longer because the weather was not as severe. Even though CSS *Parizeau* did encounter 25 m s^{-1} winds, a single microbead survived the three-week cruise, probably because much of the bow-generated spray was advected behind the sensors by the wind. However, checks on calibration stability and for salt contamination were usually negative.

It appears that the response to temperature fluctuations was limited by the enclosure. This effect accounts for the poorer than expected response and for the success of a distance constant (DC, equal to the air flow required for flushing) description of the variation of response with wind speed. Miyake *et al.* (1970) quoted a 26 Hz response at an aircraft speed

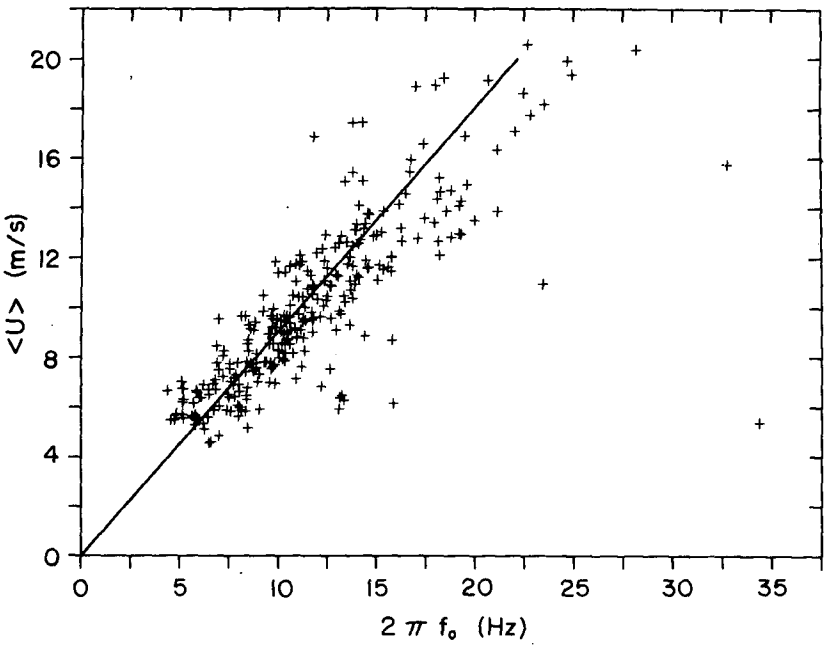

FIG. 2. Mean wind speed versus the microbead response required to equalize N_r from the 0.8 and 1.6 Hz band-pass filters at the Bedford tower. The straight line representation gives a distance constant equal to its slope of 0.90 m.

of 70 m s^{-1}, equivalent to DC = 0.4 m. In Fig. 2 the mean wind speed at the tower is plotted against the 3 db down frequency ($2\pi f_0$), assuming R-C filter behavior, required to make N_r(0.8 Hz) equal to N_r(1.6 Hz). The straight line through the origin represents a distance constant equal to its slope of 0.90 m. The data from individual microbeads agree with a DC of 0.90 m to within ±5%. Much of the scatter in Fig. 2 is likely due to real departures from the average $f^{-5/3}$ behavior.

b. The measurement of water vapor

There does not, as yet, appear to be a suitable humidity sensor for remote operation. An aluminum oxide probe (Panametrics Corp.) and a Brady array (Thunder Scientific Corp.) were tried at the tower but both deteriorated in salt air environments. *In situ* calibrations were not successful because of what may have been hysteresis effects and temperature sensitivity. Furthermore, their responses are marginal at best (Smith *et al.*, 1976).

On the ships where there were no power restrictions and where periodic servicing was possible, the fluctuating humidity was measured with a Lyman-alpha humidiometer. Remote operation on the *Quadra* was unsuccessful, because the ship-generated spray soon contaminated the tube windows. With daily cleaning and less spray, reliable data were collected at both the boom (10 m) and mast (20 m) locations on *Meteor* and from the bow of *Parizeau*. Throughout the ship operations the dewpointer provided an *in situ* calibration of the Lyman-alpha and the mean absolute humidity. Even on the foremost of CCGS *Quadra* this instrument worked reliably for more than a month without servicing. Both instruments remained operational on the *Parizeau* in winds up to 20 m s^{-1}. However, above ~15 m s^{-1} very large fluctuations were sensed by the Lyman-alpha, implying unrealistically high spectral densities and moisture fluxes. These fluctuations may have been caused by spray passing between the sensor tubes and possibly striking their windows periodically, so these data have been rejected.

A logarithmic amplifier and an inverter in the humidiometer produced a sensor voltage: $V_s = \lambda Q - \ln(V_0)$. The dry air output, $-\ln(V_0)$, did vary slowly with time, depending mainly on window transmission and contamination. The absorption parameter λ depends on path length (0.55 cm), on the absorption coefficient of water vapor and hence on the source spectrum (Buck, 1976). Using 20 min averages of $\langle Q \rangle$ from the dewpointer, it was possible to determine λ and $\ln(V_0)$, the slope and offset of calibration curves, from periods when they remained almost constant. The uncertainty in the slope, λ, proportional to $[\langle wq \rangle \mathrm{DISS}]^{-1}$, was ~ ±10%. The offset was often erratic, but it was not part of the dissipation calculations except occasionally when its variations were fast enough to pass the band-pass filters. These erroneous fluctuations were recognized by the persistence of an N_q(0.4 Hz) > N_q(0.8 Hz) > N_q(1.6 Hz) condition and the data were rejected. The response

of the Lyman-alpha system was investigated with plots analogous to Fig. 2, but no wind speed dependence was indicated, implying that the distance constant associated with the flushing of the protective housing was short enough to be ignored. Instead, the Lyman-alpha signal was assumed to be 3 db down in power at 10 Hz, because the response is at least this fast (Pond *et al.*, 1971, Buck, 1976) and because there were no consistent discrepancies between N_q(0.4 Hz), N_q(0.8 Hz) and N_q(1.6 Hz) after they were corrected for this response by 0.5, 2 and 5%, respectively. The required corrections for a 3 db down frequency of 7 Hz would have been 1, 3 and 10%, respectively, so a N_q(1.6 Hz) > N_q(0.4 Hz) condition would have persisted.

c. *The stability estimates*

Dissipation method estimates of u^*, $\langle wt \rangle$ and $\langle wq \rangle$ from 39 JASIN runs have been used to evaluate Z/L from (11), which are compared to simultaneous bulk estimates (13) in Fig. 3 (triangles). Reynolds flux u^* and $\langle wt \rangle$ values (from periods on the Bedford tower with $\Delta\theta > 0.5$ K) and an assumed 75% relative humidity have been used to find Z/L from (12), which are also compared to Z/L ($\Delta\theta$) in Fig. 3 (pluses). The cases tested in Fig. 3 suggest that the uncertainty in the bulk estimate (13) is $\sim \pm 0.05$ (considering the error in u^*, $\langle wt \rangle$ and $\langle wq \rangle$ measurements). The associated error in CT and CE (10) is only $\sim$5% near $Z/L = 0$ and it quickly lessens away from neutral stability. There are occasional large differences; points at (0.08, 0.30) and (0.15, 0.05) are beyond the range of Fig. 3. In the stable case the Reynolds flux CT values (presented in Section 4) are $\sim$20% lower, on average, than the assumed 0.75×10^{-3}, which accounts for the bias to larger bulk estimates at $Z/L > 0$. Deardorff's (1968) formulation would enhance this bias by 70% and produce $\sim$15% more unstable bulk estimates. The JASIN runs indicate that the treatment of the moisture flux in (13) is satisfactory, on average. Further testing of bulk Z/L estimates with calculations using Reynolds flux estimates of u^*, $\langle wt \rangle$ and $\langle wq \rangle$ would help to increase confidence in them. Hereafter Z/L from (13) is used exclusively, since it could always be calculated.

4. Reynolds flux, dissipation method comparison

a. *Reynolds flux results*

The reliability of the $\langle wt \rangle$FLUX results from the Bedford tower needs to be established since they are of interest in themselves and because they form the basis of the method comparison. All individual cospectral estimates from the 27 unstable and 33 stable runs were processed as described in Section 2b, to produce the normalized cospectra of Fig. 4. The overland "representative normalized cospectra for turbulent transfer" of McBean and Miyake (1972) span a wide stability range and are probably free of salt contamination. The broad spectral peak between $n = 0.02$ and 0.4 and the fall to zero between $n = 1 \times 10^{-4}$ and 4×10^{-4}, in the unstable case (Fig. 4a, $-0.35 < Z/L < 0$), are consistent with their neutral ($-0.40 < Z/L < 0.1$) and unstable ($-0.63 < Z/L < -0.46$) cospectra. With almost no covariance in unstable stratification above $n \approx 8$, there is very little high frequency distortion due to aliasing in Fig. 4a. The stable case (Fig. 4b, $0 < Z/L < 0.3$) gives cospectral values close to McBean and Miyake's (1972) neutral plot, but towards their stable curve ($4.0 < Z/L < 10.0$), at both high and low frequencies. The spectral distortion above $n \simeq 1$ in Fig. 4b indicates that most of the covariance above the Nyquist frequency is being aliased as planned. The aliased contributions are not fully corrected for sensor response, but the lost covariance should be <5% of the total in the worst case (high winds of 20 m s^{-1}).

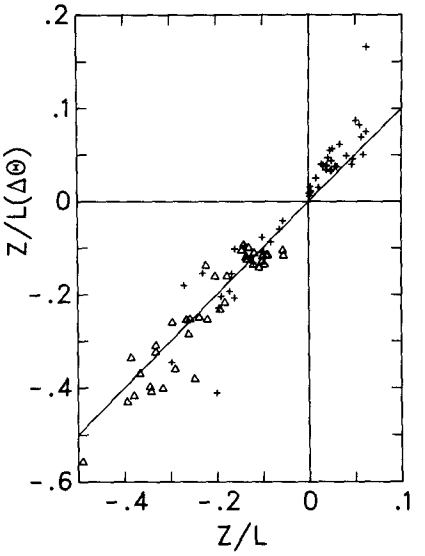

FIG. 3. Comparison of the bulk estimate of the stability parameter, $Z/L(\Delta\theta)$, to more precise calculations using eddy correlation measurements of u^* and $\langle wt \rangle$ (pluses) and dissipation method values of u^*, $\langle wt \rangle$ and $\langle wq \rangle$ (triangles). The scale for $Z/L > 0$ has been expanded for clarity.

Evaluation of $\langle wt \rangle$FLUX using (15) requires E, which has been found by integrating under the curves of Fig. 4. The plotted points are averages over bands of $\Delta \log(n) = 0.40$, while the curves are sketched to fit $\Delta \log(n) = 0.25$ band averages. It is possible to distinguish between unstable and stable stratifications, which show $E = 1.10$ and 1.04, respectively. With these values, (15) gives covariances a few percent higher, on average, than integrals that only include frequencies above 0.00065 Hz. However, over individual runs the two calculations often differ

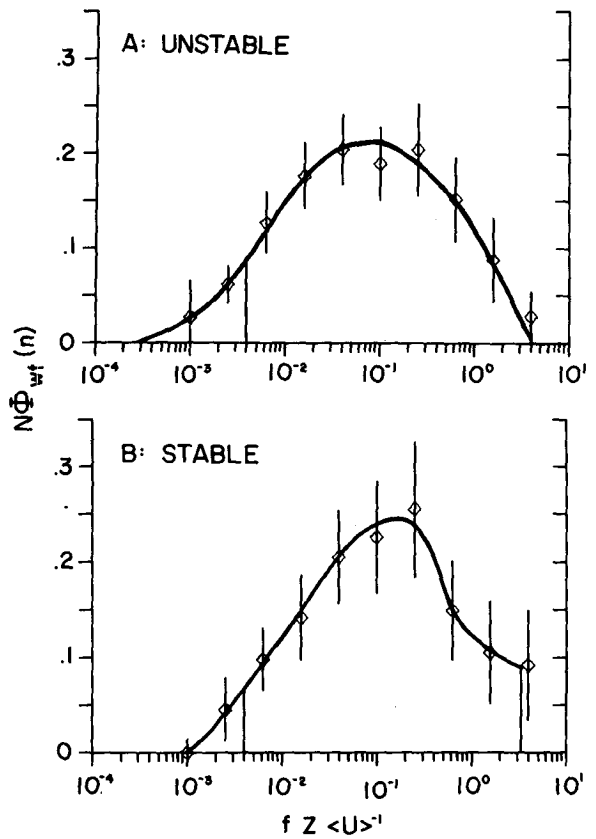

FIG. 4. Normalized w,t cospectra, $N\Phi_{wt}(n)$, from averages of

$$n \cdot \Phi_{wt}(n) \Big/ \int_{f_1}^{f_n} \Phi_{wt}(f)df$$

from 27 unstable runs (A) and 33 stable runs (B). The vertical lines extend ±1 estimate of the standard deviation of the mean. The curves are sketched to fit band averages $\log(n) = 0.25$ wide.

by 10–20%, as a consequence of poorly sampled cospectral values below $n = 0.004$, that are very different from their average relative contribution to the covariance.

The standard deviation of temperature fluctuations, σ_t, is of engineering interest and a test of the system. It has been found from integrals of the temperature spectrum from $f = 0.00065$ Hz. Normalized σ_t/t^* values [using $\langle wt \rangle$ and u^* from (15) and its analogue] averaged over bands of Z/L are presented in Table 1. Eight runs with $|Z/L| < 0.03$ have been excluded, because of the "noise" in t^* discussed by McBean (1971). Table 1 suggests that σ_t/t^* becomes smaller as the stratification becomes more unstable (as do McBean, 1971 and Wyngaard *et al.*, 1971). In the stable case, Table 1 and Wyngaard *et al.* (1971) show σ_t/t^* to be essentially constant. The means in Table 1 all fall within the scatter of the San Diego values of Phelps and Pond (1971). McBean (1971) only integrates between $n = 0.01$ and 10, and the magnitudes of his σ_t/t^* values are correspondingly smaller.

The temperature fluxes from the 52 Bedford tower runs with $|\Delta T| > 0.5$ K are plotted in Fig. 5 against $U10(T_s - \theta 10) = (U\Delta\theta)_{10}$, such that the slope from the origin to any point gives CT at 10 m (8). The solid lines are portions of Smith's (1980) regressions using ΔT, which would shift slightly to the left if $\Delta\theta$ were used. Throughout the two runs plotted as squares, very warm air moved over a cold sea and with the resulting stable water column the sea temperature measurement at a depth of 10 m may not have followed the rising sea-surface temperature, causing $\Delta\theta$ to be too negative. Nonetheless, the two $\langle wt \rangle$FLUX calculations appear to be reliable and useful for the dissipation method comparison. Near-neutral runs (crosses, $-0.1 < Z/L < 0.05$) are not distinguishable from the more stable (triangles), but the more unstable runs (pluses, $Z/L < -0.1$), although limited in number, do tend to give smaller CT's. The points of Fig. 5 generally fall within Smith's scatter, but the fit of his regression lines is not as good as expected, considering that both data sets are from the Bedford tower and both use the same sea-temperature sensor. A similar tendency for the magnitudes of BIO temperature fluxes to be larger than $\langle wt \rangle$FLUX was also noted in the Sable Island results (Smith *et al.*, 1976). This tendency persists at low wind speeds when the loss of aliased covariance in $\langle wt \rangle$FLUX is only ~2%. There is likely a sampling problem with neither Fig. 5 nor Smith (1980) being based on sufficient data to be representative of average conditions.

For the method comparison no corrections were applied to $\langle wt \rangle$FLUX, because the source of the discrepancy with Smith (1980) is unclear and because Fig. 5 is in better agreement with the results reviewed by Friehe and Schmitt (1976). The unstable points of Fig. 5 are within the scatter of their largest data set (Müller-Glewe and Hinzpeter, 1974), which extends to $(U\Delta\theta)_{10} = 30$ K m s^{-1}, and they agree with the San Diego results of Pond *et al.* (1971). In this range, a regression of the 14 runs of Fig. 5 gives $10^3\langle wt \rangle = 1.1(U\Delta\theta)_{10} - 1.0$ K m s^{-1} (correlation coefficient 0.93) compared to the $10^3\langle wt \rangle = 0.97 \times (U\Delta\theta)_{10} + 2.0$ K m s^{-1} of Friehe and Schmitt (1976). The stable points of Fig. 5, -20 K m s^{-1}

TABLE 1. The normalized standard deviation of temperature fluctuations, band-averaged over stability. Eight runs with $|Z/L| < 0.03$ have been excluded.

Mean Z/L	Runs	Mean σ_t/t^* ±1 standard deviation	Mean σ_t/T^*
−0.32	2	0.78	1.95
−0.14	11	0.99 ± 0.05	2.48
−0.08	9	1.04 ± 0.04	2.60
−0.04	3	1.30	3.26
0.04	14	1.41 ± 0.19	3.53
0.07	11	1.35 ± 0.11	3.37
0.24	2	1.57	3.93

$< (U\Delta\theta)_{10} < 0$, are within the scatter of the Hasse (1970) and the Müller-Glewe and Hinzpeter (1974) data sets in Friehe and Schmitt (1976). In the narrow range -5 K m s^{-1} $< (U\Delta\theta)_{10} < 0$, small *positive* fluxes, negative CT's, are sometimes found. The decrease to more negative temperature fluxes at more negative $(U\Delta\theta)_{10}$ values appears nearly linear, making (14) an appropriate parameterization. Correspondingly, measured CT's increase rapidly, such that (8) becomes meaningful for $(U\Delta\theta)_{10}$ more negative than ~ -25 K m s^{-1}, where the 16 usable runs of Fig. 5 give an average 10^3 CTN = 0.60 (standard deviation 0.13). In the unstable case the average 10^3 CTN from all 19 runs in Fig. 5 is 0.90 (standard deviation 0.32). The Reynolds flux data set is limited, but useful for validating the more extensive dissipation method results, which alleviate the sampling problem and provide a better opportunity to investigate the behavior and parameterization of the temperature flux.

b. *Method comparison*

In Fig. 6, simultaneous dissipation method estimates $\langle wt\rangle$DISS are plotted against the 52 $\langle wt\rangle$FLUX values of Fig. 5. These dissipation runs began less than four minutes before and finished within three minutes of the corresponding Reynolds flux runs. The solid 1:1 line differs only slightly from the regression line $\langle wt\rangle$DISS = 1.03 $\langle wt\rangle$FLUX (correlation coefficient, 0.99). The scatter is generally well within the dashed lines that bound the ±40% deviation expected because of the ±20% uncertainty in *both* methods. There is good agreement and little scatter when the flux magnitudes are largest, which are the most important situations. The fact that there is not a major systematic difference in Fig. 6 suggests that the *combined* error in the constants of (20) is not very large. The effect of the stability functions on $\langle wt\rangle$DISS (20) is less than 10% only in the narrow range $|Z/L| < 0.03$ and at more non-neutral stratification it increases rapidly, reaching 50% at $Z/L \simeq 0.15$ and -0.25. Therefore, stability modification of the mean profiles and hence to the local production of temperature variance is important, but adequately treated using $Z/L(\Delta\theta)$. The correction to $\langle wt\rangle$DISS for sensor response is a function of wind speed, but the observed agreement in Fig. 6 is not, indicating that the response is being treated satisfactorily.

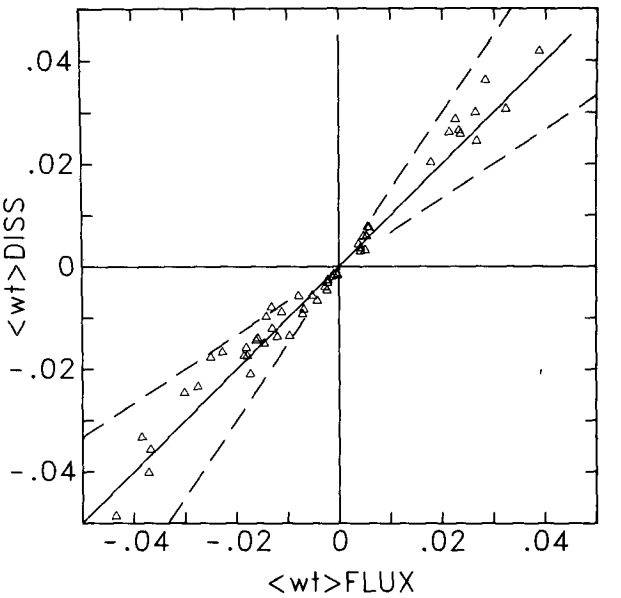

FIG. 6. Comparison of simultaneous Reynolds flux and dissipation method estimates of $\langle wt\rangle$ in K m s^{-1} from the 52 Bedford tower runs with $|\Delta\theta| > 0.5$K. Dashed lines indicate a ±40% deviation from the solid 1:1 line.

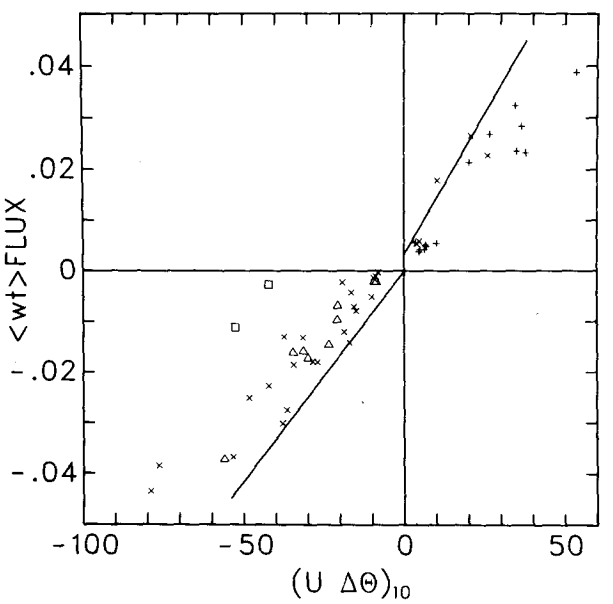

FIG. 5. Reynolds flux $\langle wt\rangle$ vs. $(U\Delta\theta)_{10}$ in K m s^{-1}, for the 52 Bedford tower runs with $|\Delta\theta| > 0.5$ K. Two suspect runs are plotted as squares. Stability ranges are: $0.05 < Z/L$ (triangles), $-0.1 < Z/L < 0.05$ (crosses) and $Z/L < -0.1$ (pluses). The solid lines are from Smith (1980).

The humidity sensors failed on the Bedford tower, where the Reynolds flux method could have been employed. However, other studies have found a favorable comparison between eddy correlation and dissipation estimates of $\langle wq\rangle$. Pond *et al.* (1971) used the same constants, but did not include the $[\phi_m(Z/L) - Z/L]^{1/6}$ term of (20); however, over their stability range, $-0.27 < Z/L < -0.11$, its effect is less than 2%. Their results are plotted in Fig. 7, demonstrating the fit of the solid 1:1 line and the reasonable scatter. These are open sea data, but only winds below 8 m s^{-1} are included. Garratt and Hyson (1975) found good agreement between 166 eddy correlation and dissipation determinations of Q^* over shallow water (4 m) in winds up to 15 m s^{-1}. They used the equivalent of (20) with $K' = 0.55$, $\beta q'$

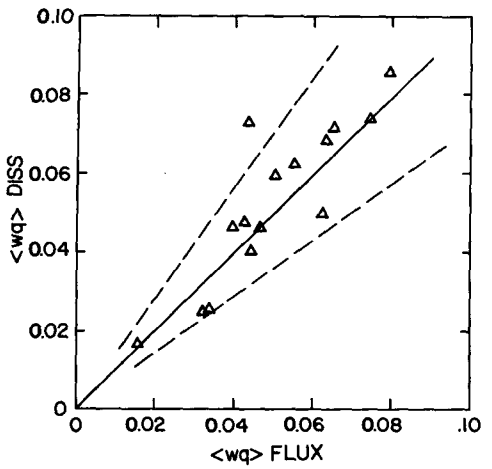

FIG. 7. Comparison of Reynolds flux and dissipation method estimates of $\langle wq \rangle$ in m s^{-1} and g m^{-3}, from the data of Pond *et al.* (1971). Dashed lines indicate a ±40% deviation from the solid 1:1 line.

= 0.80 and $\kappa = 0.41$. The BIO data from the shore of Sable Island are also showing good agreement (R. J. Anderson, pers. comm., 1981).

5. The wind measurements

The slender Bedford tower was designed not to interfere with the measurements (Smith, 1980), but careful scrutiny of the Gill anemometer data revealed that the ships seriously disturbed the air flow at certain relative wind directions, α_r (with $\alpha_r = 0$, $\alpha_r > 0$, and $\alpha_r < 0$ indicating winds over the bow, from starboard and from port, respectively). The bulk transfer coefficients (9) were calculated only when no evidence of ship interference could be found; $-90° < \alpha_r < 45°$ on CCGS *Quadra*, $|\alpha_r| < 100°$ on CSS *Parizeau*, $70° < |\alpha_r| < 120°$ when using the *Meteor* boom Gill and $|\alpha_r| < 60°$ when using the *Meteor* mast Gill. Consistent with Augstein *et al.* (1974), on *Meteor* with $|\alpha_r| < 60°$ the wind speeds at the mast and those from nearby JASIN buoys compared favorably. Simultaneously, the boom Gill measured speeds 13% lower, after adjusting for height differences and friction velocities 5 to 10% smaller than did the mast Gill. In contrast, with $70° < |\alpha_r| < 120°$ the buoys and boom Gill agreed, while the wind speeds and u^*'s at the mast were, respectively, a few percent lower and 12% smaller than at the boom. The sensors on *Quadra* were in the wake of nearby masts when $45° < \alpha_r < 120°$ or $\alpha_r \approx -90°$, and the $\Phi_u(f_c)$ did not exhibit $f^{-5/3}$ behavior. On *Parizeau*, as $|\alpha_r|$ increased beyond 100° the calculated drag coefficients would immediately increase substantially. In the case of winds from abeam, these observations are consistent with those of Shinners (1970) that above a ship the streamlines are lifted and the flow accelerated, but that forward of the bow (*Meteor* boom) the flow remains unperturbed. The winds over *Meteor* would be slower when the uplifting dominates. When the winds are head on, the observations can be interpreted as showing that streamlines are deflected a great deal horizontally [as around R/V *Flip*, Pond *et al.*, (1971)], and that well above any upstream parts of a ship (*Quadra*, *Parizeau* and *Meteor* mast locations) the flow is not seriously affected.

The ship locations of the Gill anemometers were very different, but from the relative wind directions allowed, and with Z taken as the height above the ships' water line, the ship drag coefficients were consistent with themselves and with those from the tower. The agreement between the tower and *Quadra* results extended throughout the overlapping wind speed range $8 < U10 < 20$ m s^{-1} (Large and Pond, 1981). The wind data used to calculate the heat fluxes during JASIN and from CSS *Parizeau* were a subset of those which gave the CDN's of Fig. 8a and b, respectively. The solid line was found to be a good description of the average drag coefficient from the tower and *Quadra* (Large and Pond, 1981) and it is a good fit to those from JASIN, on average. In Fig. 8a, the high values (10^3 CDN > 1.5) at low winds ($U10 < 10$ m s^{-1}) are associated with rapid changes in wind direction as was also observed at the tower. Corresponding points are absent from Fig. 8b, which accordingly displays a wind-speed dependency of CDN at all wind speeds. This is not an unexpected behavior, because almost all the low wind speed conditions occurred at the beginning of the *Parizeau* cruise, when the winds remained reasonably steady for several days and there were no rapid direction changes to produce the high coefficients at low wind speeds. Since ship and buoy mean winds agreed, the consistent behavior of the drag coefficient at all wind speeds implies that neither mean nor high-frequency flow was seriously distorted. Combining the JASIN and *Parizeau* drag coefficients with those from the tower and *Quadra* yields a data set corresponding to more than 2000 h. At all wind speeds, the additional data increase the confidence, but change band averages of CDN by 2% at most. Therefore, the combined data are also well described by the solid lines of Fig. 8

$$\left.\begin{aligned} 10^3\,\mathrm{CDN} &= 1.14 \quad 3 < U10 < 10 \text{ m s}^{-1} \\ &= 0.49 + 0.065U10 \\ &\qquad 10 < U10 < 25 \text{ m s}^{-1} \end{aligned}\right\}. \quad (21)$$

However, the average 10^3 CDN from the 950 h with $3 < U10 < 10$ m s^{-1} is only 1.12 (standard deviation, 0.20).

6. Dissipation method heat fluxes

All the reliability tests were performed on 20 min periods of dissipation data. When all three periods of an hour checked out individually, the means and

fluxes were averaged over the hour. In order to prevent errors in $\Delta\theta$ and ΔQ becoming very large in CTN and CEN, only hours with $|\Delta\theta| > 1°C$ and $\Delta Q > 1$ g m^{-3} were used to calculate the transfer coefficients, even though the fluxes were satisfactory at smaller sea-air differences. The frequent maneuvers of the *Parizeau* and *Meteor* and radio interference on the latter perturbed short intervals of some otherwise suitable hours. In these cases, only the undisturbed 20 min periods were averaged to give values representative of the hour.

a. Temperature

The dependence of the neutral Stanton number on the direction of the sensible heat flux, which for $|\Delta\theta| > 1°$ dictates the sign of Z/L, is clearly shown in Fig. 9. The pluses from the tower and the triangles from the ships are indistinguishable, on average. The sea temperature measurements were not ideal and are likely the source of much of the scatter, but averaging should reduce the effect. A few periods of microbead contamination may have escaped detection, giving erroneously high unstable CTNs. Throughout stable stratification ($\Delta\theta < 0$, downward

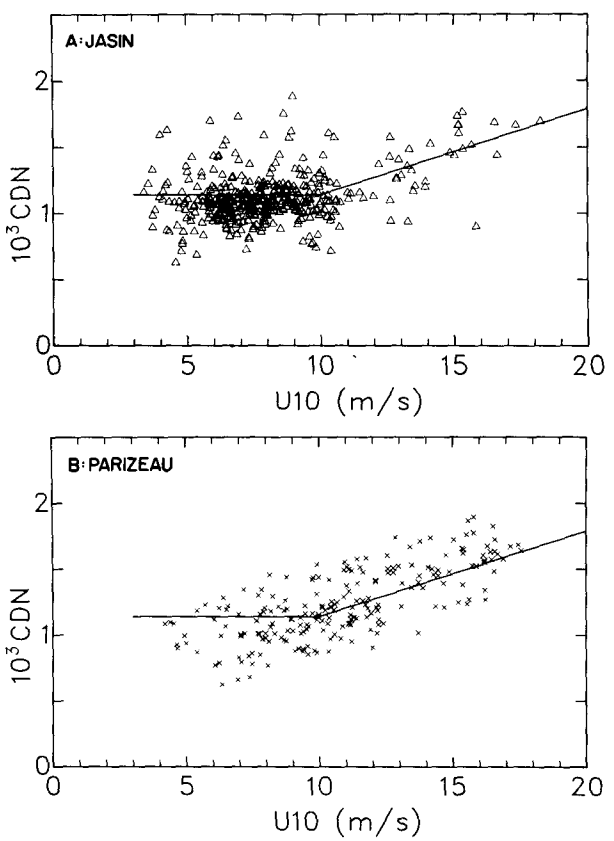

FIG. 8. The neutral drag coefficients from 400 h on F.S. *Meteor* during JASIN (A) and 180 h on CSS *Parizeau* (B) as a function of wind speed. The solid line describes the Bedford tower and CCGS *Quadra* results (Large and Pond, 1981).

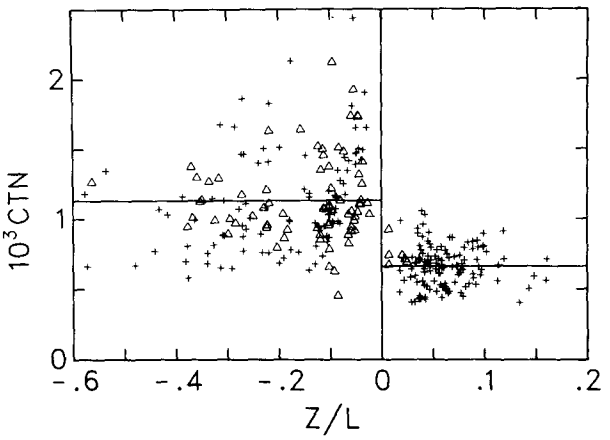

FIG. 9. The neutral Stanton numbers from the Bedford tower (pluses) and the ships (triangles) as a function of stability. The solid lines are at the overall averages in the stable and unstable cases. The scale for $Z/L > 0$ has been expanded for clarity.

temperature flux) the solid line at the overall average, 10^3 CTN = 0.66 (standard deviation of 0.14) differs from averages over Z/L bands of 0.05 by at most ±0.02. In view of the scatter in the unstable case the solid line at the overall average, 10^3 CTN = 1.13 (standard deviation 0.34), is perhaps representative. There is a tendency toward smaller CTN values at more unstable stratification, which is usually associated with lower wind speeds. The band averages of 10^3 CTN over Z/L from (−0.4 to −0.3), (−0.3 to −0.2), (−0.2 to −0.1), and (−0.1 to 0) are 0.99 (21 h), 1.14 (29 h), 1.03 (45 h) and 1.28 (56 h), respectively. The trend is neither large nor certain as all these band averages fall within ±½ of the standard deviation about the overall average. These results are compatible in the stable case and to a large extent in the unstable, with the prediction that CTN is independent of Z/L (9). However, the abrupt change at $Z/L = 0$ seen in Fig. 9 and implicitly in Fig. 5 is neither predicted nor expected. The difference is large enough to be significant, although, as discussed in Section 7, some enhancement may be due to the subsurface T_s measurements. This change has been observed to occur immediately upon a change in the sign of $\Delta\theta$ (or $\langle wt\rangle$ or Z/L). During an hour on the *Parizeau*, the air warmed quickly enough for the first 20 min period to show $\Delta\theta = 1.1$ K, $\langle wt\rangle = 0.0145$ K m s^{-1} and 10^3 CTN = 1.31 and for the third period to give $\Delta\theta = -1.0$ K, $\langle wt\rangle = -0.0093$ K m s^{-1} and 10^3 CTN = 0.65.

Since both $\langle wt\rangle$ and $(U\Delta\theta)_{10}$ are uncertain, regressions of $\langle wt\rangle$ on $(U\Delta\theta)_{10}$ and vice versa were averaged to give

$$\left.\begin{aligned}\langle wt\rangle &= 0.00074(U\Delta\theta)_{10} \\ &\quad + 0.0023 \text{ K m s}^{-1} \text{ stable, 124 h} \\ \langle wt\rangle &= 0.00106(U\Delta\theta)_{10} \\ &\quad + 0.0027 \text{ K m s}^{-1} \text{ unstable, 179 h}\end{aligned}\right\}, \quad (22)$$

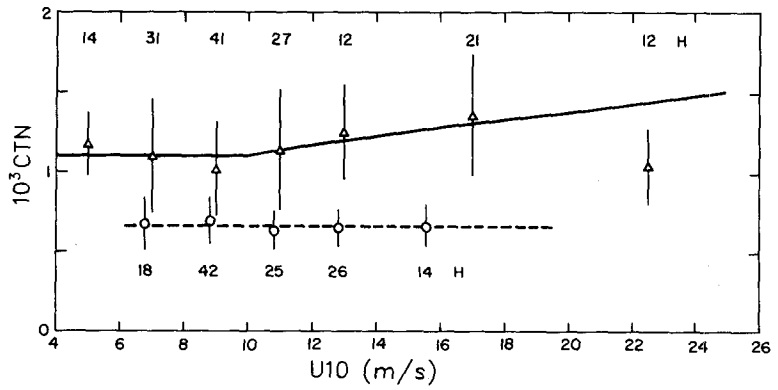

FIG. 10. An investigation of the wind-speed dependency of the neutral Stanton number in both stable (circles) and unstable (triangles) stratification. Band averages are plotted at the average $U10$, the vertical lines extend ± 1 standard deviation and the number of hours in each average are either directly above or below.

with correlation coefficients of 0.89 and 0.94, respectively. The slopes differ from the stable and unstable average CTN by 12 and 7%, respectively. Non-zero offsets are commonly observed (Müller-Glewe and Hinzpeter, 1974), implying that a bulk parameterization (8) is not appropriate for near-zero fluxes. Therefore, CTN's from $|(U\Delta\theta)_{10}| < 10$ K m s^{-1} situations have been neither plotted nor averaged. This restriction excludes situations of positive $\langle wt \rangle$ at small negative $\Delta\theta$, when the dissipation method fails, because the wrong sign is chosen for the square root of (17) or (20). The CTN values from $10 < |(U\Delta\theta)_{10}| < 20$ K m s^{-1} did not change the overall averages appreciably. The regressions (22) give larger flux magnitudes than Fig. 5, but the fit would have been better throughout if more Reynolds flux measurements had been available. This view is supported by the excellent comparison in Fig. 6, at the larger flux magnitudes where the fit of (22) to Fig. 5 is poorest. In the unstable case, the difference between Smith's (1980) stable regression and (22) [$\sim$5% at $(U\Delta\theta)_{10} = 100$ K m s^{-1}] is well within both measurement errors and possible sampling and stability biases. There is, however, a significant difference in the stable case [$\sim$18% at $(U\Delta\theta)_{10} = -50$ K m s^{-1}]. Smith's (1980) stable regression has an insignificant offset and its slope, 0.00083, should be nearly equal to the average CTN, since using $\Delta\theta$ would tend to decrease the slope, while the shift to neutral stability would increase it. This CTN is 25% higher than the average of the dissipation method, which is more than ought to be ascribed to calibration and sampling. The validity of assumptions or the values of constants used in the dissipation method may change with stability, and result in a systematic bias to smaller $\langle wt \rangle$DISS magnitudes in the less well studied stable situation. A 10% increase in the stable $\langle wt \rangle$DISS magnitudes would be within the expected error, would still give a favorable method comparison (Fig. 6) and would still give good agreement with Friehe and Schmitt (1976).

The wind speed dependency of CTN is explored separately for unstable and stable stratification in Fig. 10. The stable CTN is essentially constant at all speeds, with band averages (circles) within $\pm 0.03 \times 10^{-3}$ of the dashed line at the overall average 10^3 CTN = 0.66, which extends throughout the range of measured speeds. There is more scatter in the unstable case, but a constant CTN at the overall average, 1.13×10^{-3}, falls well within a standard deviation about all the band averages (triangles) and is in excellent agreement with Smith (1980). The 12 h of 20–25 m s^{-1} winds all come from the same storm on CCGS *Quadra*, during which average conditions may not have been realized or a measurement error, such as in T_s, may not have averaged out. The 33 unstable hours from 12 to 20 m s^{-1} display a tendency for higher CTN values at higher winds, but do not agree with the shallow water results of Francey and Garratt (1978) who found generally larger values and a stronger dependency on wind speed. Measured values of $\kappa/\ln(10\ m/Z_t)$ from *all* the unstable data average 0.0327 (standard deviation 0.010) and their averages from the lowest to highest wind speed bands in Fig. 10 are 0.0337, 0.0344, 0.0313, 0.0350, 0.0358, 0.0335 and 0.0226. There is no systematic trend, suggesting that Z_t is approximately constant at $\sim$0.0049 cm in unstable stratification. Therefore, as suggested by (9), the solid line of Fig. 10 represents

$$\mathrm{CTN} = \mathrm{CDN}^{1/2}\kappa/\ln(10\ m/Z_t), \qquad (23)$$

with CDN from (21) and $\kappa/\ln(10\ m/Z_t) = 0.0327$. It is constant at 1.10×10^{-3} at $U10 < 10$ m s^{-1} and spans the range of available measurements. Following a similar procedure in the stable case (not plotted) gives an average $\kappa/\ln(10\ m/Z_t) = 0.0180$ (standard deviation 0.009), $Z_t = 2.2 \times 10^{-7}$ cm and 10^3

CTN = 0.61 for $U10 < 10$ m s^{-1} rising to 0.70 at $U10 = 16$ m s^{-1}. Thus, (23) provides a formulation that is not very different from either the stable band averages or the dashed line in Fig. 10. Averages of $\kappa/\ln(10\ m/Z_t)$ over 2 m s^{-1} wind speed bands ranged only from 0.016 to 0.019, in the stable case.

In both the stable and unstable cases, a constant 10^3 CTN (0.66 and 1.13, respectively), a linear least-squares regression and (23) fit the data equally well, with root-mean-square (rms) differences of 0.14 $\times 10^{-3}$ and 0.35 $\times 10^{-3}$, respectively, but there is a need for independent evaluations of $\kappa/\ln(10\ m/Z_t)$. Although (23) is a better fit than 10^3 CTN = 1.13 over the range $10 < U10 < 20$ m s^{-1}, the improvement is not statistically significant. Therefore, a constant CTN may be used in both stable and unstable stratification. However, the formulation (23) is attractive, because it is consistent with (9) and it is easy to use when the more well-established CDN is also required.

b. Humidity

It has been possible to make 117 determinations of $\langle wq\rangle$DISS and the neutral Dalton number, CEN (70 from *Meteor* and 47 from *Parizeau*, corresponding to a total of 93 h). There is an uncertainty of 30–40% in individual estimates of CEN, with the Lyman-alpha calibration responsible for ~10%, along with contributions from Z/L, u^*DISS, $\langle U\rangle$ and ΔQ. Overall some cancelation is likely, leaving ~15–20% uncertainty in the average CEN, as compared to ~10% in the average CDN (Pond and Large, 1978) and average CTN. Averages of the neutral Dalton number over stability bands are presented in Table 2. The overall average, $\overline{\text{CEN}} = 1.15 \times 10^{-3}$ (standard deviation 0.22×10^{-3}) is not significantly different from any of the band averages including that from the 8 h of $-0.55 < Z/L < -0.35$. Therefore, within experimental uncertainty, the stability dependency of CE, is given by (10) and CEN is independent of Z/L, in unstable conditions. In the stable case with small downward moisture flux the results of Anderson and Smith (1981) indicate that, unlike CTN, the stable CEN is not very different from its unstable value; assuming that the influence of their onshore site is similar in both stable and unstable conditions.

TABLE 2. Averages of the neutral Dalton number over stability bands.

		10^3 CEN		
Z/L range	Hours	Mean	Standard deviation	Range
0, −0.05	33	1.18	0.26	0.67, 1.67
−0.05, −0.15	24	1.08	0.15	0.77, 1.41
−0.15, −0.35	27	1.15	0.20	0.58, 1.58
−0.35, −0.55	8	1.29		1.03, 1.60
Overall				
0, −0.55	93	1.15	0.22	0.58, 1.67

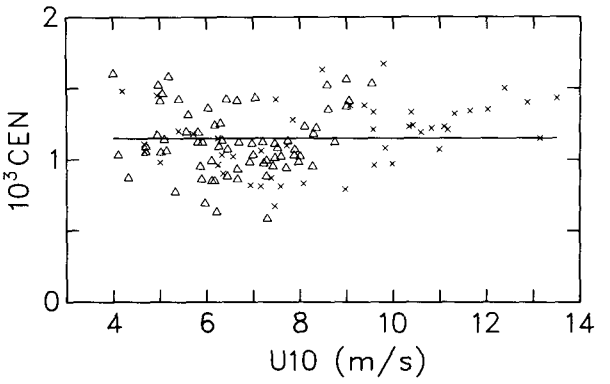

FIG. 11. The neutral Dalton numbers from 62 h on F.S. *Meteor* during JASIN (triangles) and 31 h on CSS *Parizeau* (crosses) as a function of wind speed. The solid line is at the overall average, 1.15×10^{-3}.

The neutral Dalton number is plotted against wind speed in Fig. 11. A constant at $\overline{\text{CEN}}$ (solid line) is also shown. The data from the steady wind conditions early in the *Parizeau* cruise fall into the 6–10 m s^{-1} band. Like CDN, they tend to be small and without these nine values the band average 10^3 CEN increases from 1.05 to 1.12. Above 10 m s^{-1} there are only 11 h (15 points) of data, which are insufficient to establish the behavior of CEN. However, (9) suggests using

$$\text{CEN} = \text{CDN}^{1/2}\kappa/\ln(10\ m/Z_q), \qquad (24)$$

with CDN from (21) and $\kappa/\ln(10\ m/Z_q) = 0.0346$, the overall average (standard deviation 0.006). This formulation gives 10^3 CEN = 1.17 at $U10 < 10$ m s^{-1} and 1.29 at $U10 = 14$ m s^{-1} and $Z_q = 0.0095$ cm. The five averages of $\kappa/\ln(10\ m/Z_q)$ over 2 m s^{-1} wind speed bands from 4 to 14 m s^{-1} are 0.0347, 0.0322, 0.0378, 0.0372 and 0.0392, respectively. Fits of the data in Fig. 11 to $\overline{\text{CEN}}$, a linear least-square regression and (24) all give rms differences of 0.23×10^{-3}. However, for $U10 > 10$ m s^{-1} the rms difference is 0.17×10^{-3} about $\overline{\text{CEN}}$ and 0.11×10^{-3} about both (24) and a linear regression, so to the 95% confidence level (24) is a significantly better fit than $\overline{\text{CEN}}$. The formulation (24) has the same attractions as (23); however, a constant CEN may still be used, since over our range of wind speeds (24) only changes by ~10% and because $\kappa/\ln(10\ m/Z_q)$ needs to be more firmly established.

The results of other experiments are summarized in Anderson and Smith (1981) and there is a consistency, with the exception of onshore or shallow water measurements (theirs from Sable Island; Garratt and Hyson, 1975; Francey and Garratt, 1978). Drag coefficients at similar sites also seem to differ

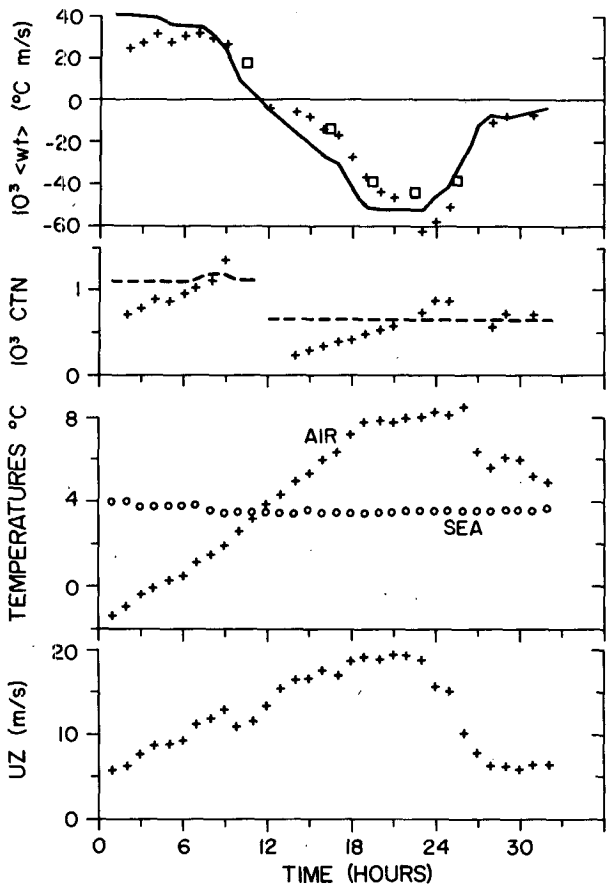

FIG. 12. Time series from 0440 GMT, 7 December 1976 at the Bedford tower. Temperature fluxes are from the Reynolds flux (squares), dissipation (pluses) and bulk aerodynamic (solid line) methods. The dashed line follows the CTN used in the bulk calculations and CTN from the dissipation data are the pluses.

from those over the deep sea (Large and Pond, 1981). The reported averages of 10^3 CEN from six other studies are between 1.05 and 1.20, which together with $\overline{CEN} = 1.15 \times 10^{-3}$, suggest that errors, especially in calibration, have tended to cancel and that the uncertainty in CEN is somewhat less than 20%. The agreement between midlatitude and tropical experiments is well within experimental error, so the parameterization of $\langle wq \rangle$ in terms of $(U\Delta Q)_{10}$, (8), seems appropriate in both regions. Pond *et al.* (1971) quote an average CE = 1.23×10^{-3} for eddy correlation measurements at 8 m and unstable, $-0.40 < Z/L < -0.10$, conditions and Fig. 7 shows that their dissipation results are very similar. The shifts to neutral stability and 10 m height are ~10 and 5%, respectively, such that the mean 10^3 CEN is ~1.07. At their tropical BOMEX site large fluxes were due to large sea-air humidity differences, ΔQ, up to 9 g m^{-3}. For similar tropical conditions and winds to 11 m s^{-1} during ATEX, Dunckel *et al.* (1974) found CE at 10 m height to average 1.28 $\times 10^{-3}$. Adjustment to neutral stability would likely give 10^3 CEN < 1.20. During our midlatitude experiments ΔQ never exceeded 4 g m^{-3} and large fluxes were due to high winds.

A regression of our 117 points gives a correlation coefficient of 0.92 and

$$\langle wq \rangle = 0.00142(U\Delta Q)_{10} - 0.035 \text{ g m}^{-3} \text{ m s}^{-1}. \quad (25)$$

The slope is 23% larger than $\overline{CEN}$ because of the negative offset and stability bias and should not be equivalenced to a transfer coefficient (8). Friehe and Schmitt (1976) recommend CE = 1.32×10^{-3}, which is the slope of a regression with a negative offset of -0.0026 g m^{-3} m s^{-1}. However, their average CEN would be close to 1.1×10^{-3}, since 20 of their 30 points come directly from Pond *et al.* (1971) as $(U\Delta Q)$ at 8 m.

7. Time variability

When nearly continuous data were available for more than a day, time histories of the direct measurements and derived quantities were constructed. They showed that much of the observed scatter in individual transfer coefficients was not random and revealed potential problems with some of the data. They also provided a detailed comparison of the bulk and dissipation methods.

Fig. 12 displays time series of Bedford tower measurements. Corresponding series of CDN and additional parameters are presented in Large and Pond (1981). The $\langle wt \rangle$ series compare the dissipation (pluses), the Reynolds flux (squares) and the bulk (solid line) methods. CTN for $\langle wt \rangle$BULK was found from (23) in unstable conditions and assumed constant at 0.00066 in stable (dashed lines). During the previous 12 h there was little wind and an air temperature of -15°C, $\Delta\theta \approx 20$°C. Although CTN varies by a factor of 2 in both stable and unstable periods, it is a relatively smooth function of time, as is CDN. Over the first 10 h, the unstable CTN increases with wind speed and the rising wind conditions result in CTN, like CDN, being lower than the average as represented by the dashed line. The rapid fall of wind speed after hour 23 was accompanied by an almost 180° shift in wind direction. This situation produced very large drag coefficients, but the stable CTN is not very different from its average. Following the transition to stable stratification at hour 10 there is a large decrease in CTN, which then increases as the wind speed continues to rise. However, this is the situation discussed in Section 4, when the T_s measurement at depth may have been inadequate. The effect on CTN is evident and neither Figs. 9 and 10 nor the regressions (22) contain these data, to hour 22. Nonetheless, the eddy correlation and dissipation calculations seem to be reliable and were used in Fig. 6. Erroneously small CTN values

from similar, but less extreme circumstances may be included in the stable values of Fig. 9. However, the corresponding effect during atmospheric cooling and unstable stratification (low CTN's due to a sea-temperature increase with depth) would likely be much less because of the unstable nature of the vertical sea-temperature gradient. It is possible, therefore, that the Bedford tower sea-surface temperature measurement at 10 m depth somewhat enhanced the difference between the average stable and unstable CTN, as seen in Fig. 9.

Fig. 13 contains the time series of four days during JASIN when numerous simultaneous sensible and latent heat fluxes are available. Throughout this time the wind blew from the north ±40°, there was unstable stratification and the air density, sea temperature and air temperature were 1.24 kg m^{-3}, 13.5 ± 0.2°C and 11.5 ± 1.0°C, respectively. The dissipation method estimates (pluses) can be compared to bulk estimates (solid curves), based on average bulk transfer coefficients in these conditions. Relative to their average, high or low calculated coefficients are reflected by the pluses falling, respectively, above or below the solid curves. The cumulative fluxes over this period give H_s BULK > H_s DISS and H_L BULK < H_L DISS, though the differences, as a percentage of the total are not large. Over the order of a day, there are, however, significant systematic discrepancies between the two methods. Errors in neither the dissipation method nor bulk measurements are expected to persist so long (note the higher-frequency variability in all the time series). Instead, some of the observed scatter in CEN and CTN measurements, like that of CDN, may be real, because possible sources, such as wind-wave effects may be of this time scale. Bulk estimates using average coefficients would be insensitive to such variability, which could account for some of the differences in Fig. 13, but any effect appears to be minimal on averages over a few days.

The time series reveal some potential measurement problems that could cause discrepancies between the results from small data sets. Fig. 12 shows how serious errors could persist for several hours and Fig. 13 indicates that average conditions may not be realized in a day. Therefore, the disagreement between (23), unstable and the 12 hours of 20–25 m s^{-1} data from CCGS *Quadra* could be a sampling problem. A bias could be present in the 15 estimates of CEN at winds above 10 m s^{-1} in Fig. 11.

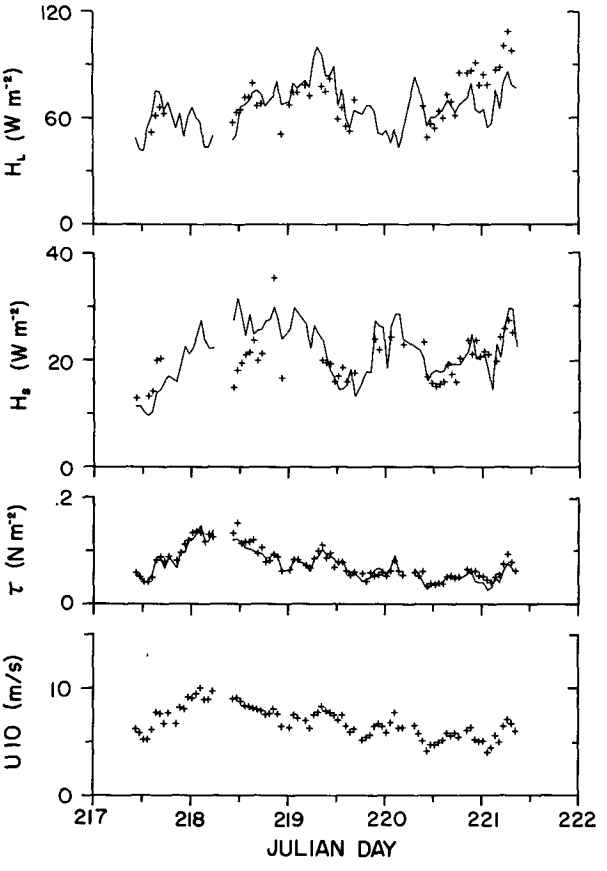

FIG. 13. Time series of the turbulent fluxes of momentum, sensible heat and latent heat from the dissipation (pluses) and bulk aerodynamic (solid line) methods during JASIN, 1978.

8. Discussion and conclusion

It has been demonstrated that the turbulent heat fluxes, like the momentum flux, can be measured from ships on the deep sea, by the dissipation techniques. However, care must be taken to avoid locations of ship-generated spray and flow distortion. Our system provided automated, but as yet neither routine nor remote, shipboard measurements. Microbead salt contamination was a serious problem and a measure of low-frequency temperature variance to compare with values in the $f^{-5/3}$ region was required for its diagnosis. The *in situ* dewpointer calibration of the Lyman-alpha was successful. The height of the *Parizeau*'s humidiometer appears to have limited reliable measurements of the water vapor fluctuations to winds below 15 m s^{-1}. The response of the microbeads was limited by their protective housing, but it was satisfactorily modeled with a distance constant of 0.90 m. Small corrections were required for the humidiometer response.

The simultaneous dissipation and eddy correlation estimates of $\langle wt \rangle$ from the Bedford tower compared favorably, especially when the flux was large either upwards or downwards. The normalized stable and unstable w,t cospectra were compatible with those of other studies as were values of the normalized temperature variance. These cospectra indicated that $\langle wt \rangle$FLUX could be obtained by integrating an unstable or stable $\Phi wt(n)$ from n = 0.004 then multi-

plying by 1.10 or 1.04, respectively. This was a means of preserving covariance, on average, while avoiding some large, poorly sampled low-frequency contributions. The magnitudes of these fluxes and the calculated transfer coefficients were in reasonable agreement with Friehe and Schmitt (1976), but tended to be smaller than those of Smith (1980). The discrepancies were largely attributable to sampling biases in the small data sets, because of the better agreement of the larger dissipation data set. A linear regression gave $\langle wt\rangle$DISS = 1.03 $\langle wt\rangle$FLUX, thus the two methods did not significantly differ. This agreement and the results of other works, which indicated that $\langle wq\rangle$DISS could be similarly calculated, verified the dissipation method, or if preferred, established (20) as an appropriate parameterization, with S_E and S_T as given by theory and measurement. The uncertainty in the dissipation fluxes and transfer coefficients was of the same order as in eddy correlation calculations (10% and 15–20% in the average CTN and CEN, respectively).

The dissipation measurements have significantly increased the deep-sea CTN and CEN data sets. There was considerable scatter in unstable stratification, but a reasonable representation was the average 10^3 CTN = 1.13 ± 10% in 4 to 25 m s^{-1} winds. The majority of data above 10 m s^{-1} exhibited a weak wind-speed dependency that could be incorporated with CTN = CDN$^{1/2}\kappa$/ln(10 m/Z_t) in all winds. Averages of unstable κ/ln(10 m/Z_t) were nearly independent of wind speed with an overall average of 0.0327. In stable stratification, downward temperature flux, there was comparatively little scatter in CTN and its mean, 0.66×10^{-3}, was a good fit to the data, with no wind-speed dependency in 6–20 m s^{-1} winds. The CDN$^{1/2}$ dependence was weak and fit the data equally well. This study and Smith (1980) show the Stanton number to be smaller in the stable case, with 10^3 CTN = 0.75 within ±0.10 of both results. It was noted that a CTN parameterization was not appropriate at small fluxes $|(U\Delta\theta)_{10}|$ less than 10–20 K m s^{-1}. Instead, considering all the available data, (14) with $a_t \approx 1.0 \times 10^{-3}$ and $b_t \approx 0.002$ K m s^{-1} for $\Delta\theta > 0$, and $a_t \approx 0.8 \times 10^{-3}$ and $b_t \approx 0.002$ K m s^{-1} for $\Delta\theta < 0$, may be used.

The deep-sea CEN was not measured in stable stratification. In the unstable case, there was considerable uncertainty in all the available results, but they place CEN in the range 1.05 to 1.20×10^{-3}. Our data were well described by their overall average 10^3 CEN = 1.15, which agreed with other deep water results to well within its uncertainty. The fit to the few higher wind-speed measurements was improved with a CEN = 0.0346CDN$^{1/2}$ formulation (24), where the constant was the average of κ/ln(10 m/Z_q).

For his computations of the water vapor flux of the North Atlantic, Bunker (1976) used a wind-speed-dependent neutral CE, that was nearly equal to (24) for winds below 6 m s^{-1} or above 25 m s^{-1}, but about 20% higher for 10 m s^{-1} winds. He then increased his values by 10% to correct for suspected flow distortion around the reporting merchant ships, though such a correction does not appear to be needed at all relative wind directions. The results of this present study indicate that Bunker overestimated CE and hence the flux, but only by 10–20% (depending on the wind statistics). He also assumed CT = CE, which would greatly overestimate the downward sensible heat flux in stable stratification, but the effect on the total heat flux would be small. Since routine measurements of surface stress and u^* may become available from satellite scatterometers (Liu and Large, 1981) or ambient acoustical noise in the ocean (Shaw *et al.*, 1978), (2) and (4) give appropriate parameterizations of the heat fluxes to be

$$\langle wt\rangle = \kappa u^* \Delta\theta[\ln(Z/Z_t) - \psi_t(Z/L)]^{-1},$$

$$\langle wq\rangle = \kappa u^* \Delta Q[\ln(Z/Z_q) - \psi_q(Z/L)]^{-1}.$$

The quantities ln(10 m/Z_t) and ln/(10 m/Z_q) appear to be constants, on average, and if they become more firmly established heat fluxes could be determined from these formulas perhaps more accurately than from (8) and (10) because the stability influence is less, scatterometer wind speed and u^* values are equally good and probably better than routine ship observations (Liu and Large, 1981) and the variability of Z_0 is accounted for through u^*. The study of Esbensen and Reynolds (1981) indicates that, at least over much of the North Atlantic and North Pacific oceans, monthly means of ΔQ and $\Delta\theta$, possibly from ships, would be sufficient to determine monthly averaged heat fluxes.

Time series of the fluxes indicated significant differences between bulk and dissipation heat fluxes that persisted over the order of a day. The bulk estimates were held to be responsible for much of this disagreement. They depend only on wind speed, $\Delta\theta$ or ΔQ and to a lesser degree Z/L, so they cannot respond to factors such as changing wind-wave conditions that may effect CTN and CEN. Additionally, some large errors in T_s were suspected. However, accurate heat fluxes averaged over a few days were expected from the bulk method. If much of the variability in calculated transfer coefficients is real, then theories and formulation describing their behavior are applicable only when factors not accounted for are averaged out. The average CTN depended critically on the sign of the sensible heat flux, which lacks a theoretical explanation. Otherwise, the stability dependence of CT and CE was well described by similarity theory (10). Well within the uncertainty in their averages at winds below 10–12 m s^{-1}, CDN (or Z_0), CEN (or Z_q) and CTN (or Z_t) in unstable stratification were equal and constant. The

stable CTN (or Z_t) was also independent of wind speed. For higher winds the results were equally well represented by CEN and both CTN's constant as by Z_q and both Z_t's constant, with the $CDN^{1/2}$ wind-speed dependencies predicted by similarity theory (9). The difference between the two formulations was small compared to experimental error and there were insufficient data to determine which was better. Averages of CEN and CTN, as functions of wind speed, did not agree qualitatively or quantitatively with the model of Liu *et al.* (1979), which shows CEN and CTN to be a maximum of about 1.4×10^{-3} at 5 m s^{-1}, and to decrease to about 1.1×10^{-3} at 20 m s^{-1}. This model and Friehe and Schmitt (1976) indicate that CE should be ~15% larger than CT, because the Prandtl number is larger than the Schmidt number, but this difference was too small to be resolved.

Acknowledgments. This work was supported by the United States Office of Naval Research (Contracts N 00014-66-C-0047 and N 00014-76-C-0046 under Project 083-207) and by the National Research Council of Canada (Grant A 8301). W. G. Large received personal support from ONR, NRC and the University of British Columbia.

We are grateful for the assistance provided by Dr. S. D. Smith and the air-sea interaction group at the Bedford Institute of Oceanography. The cooperation of the officers and crews of CCGS *Quadra*, F.S. *Meteor* and CSS *Parizeau* was essential for the ship operations. The efforts of the technical staff at Oceanography, University of British Columbia, particularly of E. Meyer, D. English, B. Walker and H. Heckl are gratefully acknowledged. Our thanks to the Institute of Oceanographic Sciences, Wormley, England for providing the facilities for processing the JASIN data.

REFERENCES

Anderson, R. J., and S. D. Smith, 1981: Evaporation coefficient for the sea surface from eddy flux measurements. *J. Geophys. Res.*, **86**, 449-456.

Augstein, E., H. Hober and L. Krügermeyer, 1974: Fehler bei Temperatur-, Feuchte- und Windmessungen auf Schiffen in tropischen Breiten. *"Meteor"-Forschungs-Ergebnisse*, Reihe **9**, 1-10.

Bradley, E. F., R. A. Antonia and A. J. Chambers, 1981: Temperature structure in the atmospheric surface layer. I. The budget of temperature variance. *Bound.-Layer Meteor.*, **20**, 275-292.

Buck, A. L., 1976: The variable-path Lyman-alpha hygrometer and its operating characteristics. *Bull. Amer. Meteor. Soc.*, **57**, 1113-1118.

Bunker, A. F., 1976: Computations of surface energy flux and annual air-sea interaction cycles of the North Atlantic Ocean. *Mon. Wea. Rev.*, **104**, 1122-1140.

Busch, N. E., 1977: Fluxes in the surface boundary layer over the sea. *Modelling and Prediction of the Upper Layers of the Oceans*, E. B. Kraus, Ed., Pergamon Press, 72-91.

Businger, J. A., 1982: The fluxes of specific enthalpy, sensible heat and latent heat near the earth's surface. *J. Atmos. Sci.* **39**, (in press).

Champagne, F. H., C. A. Friehe, J. C. LaRue and J. C. Wyngaard, 1977: Flux measurements, flux estimation techniques and fine-scale turbulence measurements in the unstable surface layer over land. *J. Atmos. Sci.*, **34**, 515-530.

Deardorff, J. W., 1968: Dependence of air-sea transfer coefficients on bulk stability. *J. Geophys. Res.*, **73**, 2549-2557.

Dunckel, M., L. Hasse, L. Krügermeyer, D. Schriever and J. Wucknitz, 1974: Turbulent fluxes of momentum, heat and water vapor in the atmospheric surface layer at sea during ATEX. *Bound.-Layer Meteor.*, **6**, 81-106.

Dyer, A. J., 1974: A review of flux-profile relationships. *Bound.-Layer Meteor.*, **7**, 363-372.

Esbensen, S. K., and R. W. Reynolds, 1981: Estimating monthly averaged air-sea transfers of heat and momentum using the bulk aerodynamic method. *J. Phys. Oceanogr.*, **11**, 457-465.

Francey, R. J., and J. R. Garratt, 1978: Eddy flux measurements over the ocean and related transfer coefficients. *Bound.-Layer Meteor.*, **14**, 153-166.

Friehe, C. A., and K. F. Schmitt, 1976: Parameterization of air-sea interface fluxes of sensible heat and moisture by bulk aerodynamic formulas. *J. Phys. Oceanogr.*, **6**, 801-809.

Garratt, J. R., and P. Hyson, 1975: Vertical fluxes of momentum, sensible heat and water vapor during the Air Mass Transformation Experiment (AMTEX) 1974. *J. Meteor. Soc. Japan*, **53**, 149-159.

Hasse, L., 1970: On the determination of vertical transports of momentum and heat in the atmospheric boundary layer at sea. Tech. Rep. 188, Dept. of Oceanogr., Oregon State University, 55 pp.

——, M. Gruenewald and D. E. Hasselmann, 1978: Field observations of air flow above the waves. *Turbulent Fluxes Through the Sea Surface, Wave Dynamics, and Prediction*, A. Favre and K. Hasselmann, Eds., Plenum Press, 483-494.

Large, W. G., 1979: The turbulent fluxes of momentum and sensible heat over the open sea during moderate to strong winds. Ph.D. thesis, Inst. Oceanogr. and Dept. Physics, University of British Columbia, 180 pp.

——, and S. Pond, 1981: Open ocean momentum flux measurements in moderate to strong winds. *J. Phys. Oceanogr.*, **11**, 324-336.

Liu, W. T., and W. G. Large, 1981: Determination of surface stress by Seasat-SASS: A case study with JASIN data. *J. Phys. Oceanogr.*, **11**, 1603-1611.

——, K. B. Katsaros and J. A. Businger, 1979: Bulk parameterization of air-sea exchanges of heat and water vapor including the molecular constraints at the interface. *J. Atmos. Sci.*, **36**, 1722-1735.

McBean, G. A., 1971: The variation of the statistics of wind temperature and humidity fluctuations with stability. *Bound.-Layer Meteor.*, **1**, 438-457.

——, and M. Miyake, 1972: Turbulent transfer mechanisms in the atmospheric surface layer. *Quart. J. Roy. Meteor. Soc.*, **98**, 383-393.

Miyake, M., M. Donelan and Y. Mitsuta, 1970: Airborne measurements of turbulent fluxes. *J. Geophys. Res.*, **75**, 4506-4518.

Müller-Glewe, J., and H. Hinzpeter, 1974: Measurements of the turbulent heat flux over the sea. *Bound.-Layer Meteor.*, **6**, 47-52.

Paquin, J. E., and S. Pond, 1971: The determination of the Kolmogoroff constants for velocity temperature and moisture from second and third order structure functions. *J. Fluid Mech.*, **50**, 257-269.

Paulson, C. A., 1970: Representation of wind speed and temperature profiles in the unstable atmospheric surface layer. *J. Appl. Meteor.*, **9**, 857-861.

Phelps, G. T., and S. Pond, 1971: Spectra of the temperature and humidity fluctuations and of the fluxes of moisture and sensible heat in the marine boundary layer. *J. Atmos. Sci.*, **28**, 918-928.

Pond, S., and W. G. Large, 1978: A system for remote measurements of air-sea fluxes of momentum, heat and moisture during moderate to strong winds. Manuscript Rep. No. 32, Inst. Oceanogr., University of British Columbia, 55 pp.

——, G. T. Phelps, J. E. Paquin, G. A. McBean and R. W. Stewart, 1971: Measurements of the turbulent fluxes of momentum moisture and sensible heat over the ocean. *J. Atmos. Sci.*, **28**, 901–917.

——, W. G. Large, M. Miyake and R. W. Burling, 1979: A Gill twin propeller-vane anemometer for flux measurements during moderate and strong winds. *Bound.-Layer Meteor.*, **16**, 351–364.

Roll, H. U., 1965: *Physics of the Marine Atmosphere.* Academic Press, 426 pp.

Schmitt, K. F., C. A. Friehe and C. H. Gibson, 1978: Humidity sensitivity of atmospheric temperature sensors by salt contamination. *J. Phys. Oceanogr.*, **8**, 151–161.

Shaw, P. T., D. R. Watts and H. T. Rossby, 1978: On the estimation of oceanic wind speed and stress from ambient noise measurements. *Deep-Sea Res.*, **25**, 1225–1233.

Shinners, W. W., 1970: Status of instrument development for specialized marine observations. *Meteor. Monogr.*, No. 33, Amer. Meteor. Soc., 294–301.

Smith, S. D., 1980: Wind stress and heat flux over the ocean in gale force winds. *J. Phys. Oceanogr.*, **10**, 709–726.

——, R. J. Anderson, E. G. Banke, E. P. Jones, S. Pond and W. G. Large, 1976: A comparison of the air–sea interaction flux measurement systems of the Bedford Institute of Oceanography and the Institute of Oceanography, University of British Columbia. Bedford Inst. Oceanogr. Rep. Ser., BI-R-76-17, 41 pp.

Williams, R. M., and C. A. Paulson, 1977: Microscale temperature and velocity spectra in the atmospheric boundary layer. *J. Fluid Mech.*, **83**, 547–567.

Wyngaard, J. C., and O. R. Coté, 1971: The budgets of turbulent kinetic energy and temperature variance in the atmospheric surface layer. *J. Atmos. Sci.*, **28**, 190–201.

——, O. R. Coté and Y. Izumi, 1971: Local free-convention, similarity and the budgets of shear stress and heat flux. *J. Atmos. Sci.*, **28**, 1171–1182.

Yaglom, A. M., 1977: Comments on wind and temperature flux-profile relationships. *Bound.-Layer Meteor.*, **11**, 89–102.